

Impact of satellite degraded attitude on ERS-2 Scatterometer data

°M. Sunda, °° R. Crapolicchio, °°°P. Lecomte

° Universita' degli Studi di Cagliari, Dipartimento di Ingegneria Elettrica ed Elettronica,
Piazza D'Armi, 09123, Cagliari, Italy e-mail: Sunda@diee.unica.it

°° SERCO s.p.a. via Sciadonna 24, 0044 Frascati, Italy e-mail: Raffaele.Crapolicchio@esa.int

°°° ESA/ESRIN via Galileo Galilei, 00044 Frascati, Italy e-mail: Pascal.Lecomte@esa.int

ABSTRACT

Since 17th January 2001 a gyro-less Attitude and Orbit Control System (AOCS) is used to pilot the ERS-2 satellite. The scope of this new AOCS is to increase the mission safety, after the lost of 5 of the 6 gyroscopes. With this new AOCS configuration (named as: Zero Gyro Mode – ZGM) the satellite attitude is degraded in particular for the yaw angle. The antenna mispointing could not be corrected in the existing ground processor, which assumed a very high accuracy in the satellite attitude ($\pm 0.2^\circ$). As consequence the backscattering coefficients derived from the returned echoes are not calibrated anymore. For that reason a complete review of the Scatterometer processor became necessary to insure the continuity of the Scat ERS-2 mission with the nominal high data quality. The scope of this paper is to present the impact of attitude error angles in the Scatterometer data quality. The paper also addresses the main reasons of that degradation (large frequency shift of the returned echoes, bandwidth of the on board receiver) and gives the first input for a review of the ERS-2 Scatterometer ground processing.

Keywords: Scatterometer, Attitude, Yaw

1. INTRODUCTION

The Scatterometer instrument on board ERS satellites is a three antennae side looking active microwave sensor (C-Band). The three antennae mounted on the top of the satellite provide backscattering measurements with respect to the satellite velocity, 45° foreward, sideways and 45° backwards of the Earth surface. The swath of approximately 500 km width is parallel to the subsatellite track. Inside the swath a regular grid of points, called measurement nodes, is defined and the spacing of which is approximately 25 km. For each antenna a σ^0 measurement is associated to each node, after a weighted average of backscattering coefficients of the samples neighborhood of that node. The received

echo from a target on the Earth's surface doesn't always have the same frequency as the transmitted signal because of Doppler effect due to relative motion between satellite and target. The frequency shift of the received signal depends on satellite attitude (position and velocity), antenna look angle, and Earth and target motion. The range of the Doppler shift with a sun synchronous orbit like ERS satellite is 20 - 150 KHz for the side antennae (Fore and Aft) and 0 - 10 KHz for the Mid antenna. In nominal condition the Mid beam Doppler shift is minimized by yaw steering the satellite. This aims to match the projected roll satellite axis (the reference one for the antenna mounting angle) on the tangential plane on earth model surface (GEM6) at the geodetic subsatellite point with the projected relative velocity vector. The harmonic rotation applied about the yaw axis (aligned to the local normal of the earth reference ellipsoid) is shown in Fig 1. The maximum of the correction (roughly 4 degrees) is applied at the ascending and descending crossing node. The Fore and Aft Doppler frequency shifts are minimized by continuous tuning of the receiver in order to keep the spectrum within the 25 KHz of on-board bandwidth (Doppler compensation). The required tuning signal is synthesised on-board by the Scatterometer electronic module, using a time dependent algorithm (both in orbit time and echo time) with coefficient provided to the instrument by macrocomand from the on-ground satellite control centre. The control of the attitude of the platform during the nominal Yaw Steering Mode (YSM) is autonomous (it requires only one sequence of memory loading per day in order to reset all ephemeris or other parameters) and is performed inside the Attitude and Orbit Control System module (AOCS). The nominal ERS AOCS configuration includes a Digital Earth Sensor (DES), a Digital Sun Sensor (DSS) and a triplet of gyroscopes. During the ERS-2 mission the AOCS was re-configured due to gyroscopes failure. In particular at the beginning of February 2000 three of six available gyroscopes were out of order or very noisy. In that condition was not more safe to pilot the satellite with only the last three gyroscopes and on 7th February

2000 was implemented a new AOCS schema able to pilot the satellite with only 1 gyro, the DSS and DES. The new configuration named Mono-gyro (MGM) aimed to extend the satellite lifetime using the available gyroscope one at a time. The implementation of the MGM was successful and no degradation in the ERS payload data quality was detected. On 7th October 2000 a failure of gyroscope number 5 caused to switch to gyroscope number 6 (gyro-6) and on 25th October 2000 the last available gyroscope (the number 1) was put in service after the failure of gyro-6. In order to preserve the remaining gyroscope for further satellite orbit manoeuvres, since 7th June 2001 the ERS-2 spacecraft is piloted without any gyroscopes. This last AOCS configuration is named Zero Gyro Mode (ZGM) and it had an impact in the Scatterometer mission. The accuracy with the received signals are actually centered within the receiver band depends on many factors such as the pointing errors, the receiver hardware errors, the computational and curve-fitting errors (for the on-board Doppler compensation) as well as uncertainties introduced by the geometry such as Earth and orbit modelling. These errors have an effect on instrument radiometric stability. In particular for the pointing errors, the ZGM AOCS configuration is not able to meet anymore the initial requirements for the yaw angle. Those requirements are reported in Table 1^[1].

Table 1 AOCS Pointing Accuracy Requirements

Axis	Bias & Long Term Drift	Harmonic and random Statistical 3 σ
Pitch	0.14°	0.066°
Roll	0.14°	0.082°
Yaw	0.21°	0.1°

At the beginning of AOCS ZGM operations the yaw errors were up to ± 10 degrees (peak to peak) and then, after roughly six months of commissioning phase, was reached an error of ± 2 degrees (peak to peak). As consequence since the beginning of the ZGM activities the retrieved backscattering coefficients are not calibrated and wind data are not distributed to the users.

The paper aims to describe and model the causes that had contributed to data degradation both on-board and on ground processor. The paper is organised as follows. The next section describes the impact of an error in the yaw angle in the Scatterometer received signal and reports on theoretical limit about the applicability of a possible yaw compensation in the ground processing. Section III presents the impact of the yaw error angle in the radar equation and therefore in the computation of the calibration coefficients as well as the localization errors of the echo samples. Section IV concludes the paper and summarises the most important achievements. In Section V are the references.

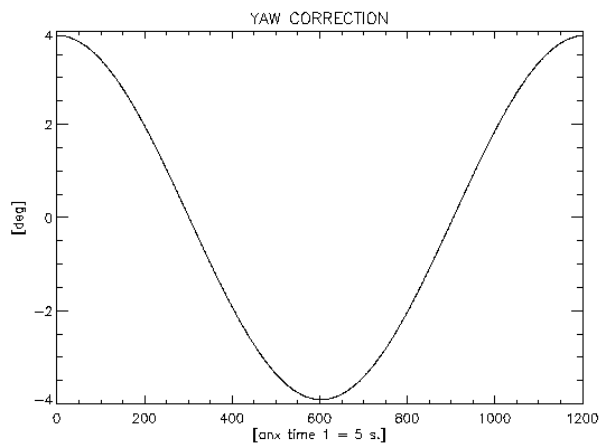


Fig. 1. ERS Yaw angle control law. On x-axis is reported the orbit time. Each unit corresponds to 5 seconds. Due to the relative motion between satellite and Earth surface the maximum correction is applied at the ascending node (unit = 0) and at the descending node crossing (unit = 600 corresponding to 3000 seconds roughly 50 minutes after the ascending node).

2. MODIFICATION OF THE RECEIVED SPECTRUM

2.1 Description of Scatterometer receiver

In Fig. 2 is shown as block diagram the Scatterometer transmitter and receiver chain. The echo signal is received by the appropriate antenna and fed into the receiver low noise amplifier. The amplified signal is then down converted to an intermediate frequency and finally demodulated by an I-Q detector (coherent detector). Due to the relative motion between satellite and target, the signal is Doppler shifted therefore the local oscillator signals for the I-Q detector are offset in frequency according to the expected shift. The compensation law is time dependent (orbit time and echo time) with coefficients provided by macrocomands. The coefficients are updated every 15 seconds but provision are made that no update takes place during the 32 pulses sequences of a single beam. Due to the fact that the Doppler frequency shift is remarkably changing over the orbit the on-board Doppler compensation is only a coarse one, whereas the fine Doppler correction is performed in the ground processing. Without any correction, the received spectrum for the Fore and Aft beam would be completely out of the passband of the low pass filters (25KHz) following the I-Q detector. After the low pass filters the signals are analogue to digital converted (each 8 bit) with a sampling rate of 30KHz and delivered to the Instrument Data Handling and Transmission (IDHT) subsystem for temporary storage and transmission to the ground.

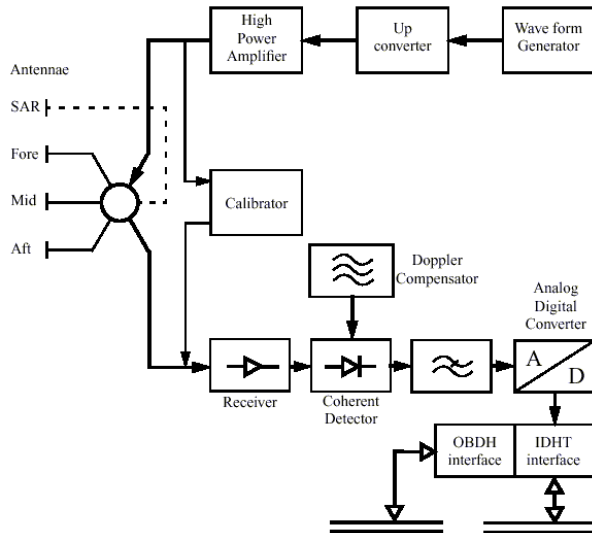


Fig. 2. ERS Scatterometer Transmitter and Receiver chain.

2.2 Modelisation of Doppler frequency evolution across track for different yaw error angles

The on-board Doppler compensation is performed taking into account the nominal satellite - target geometry that follows from a free error piloting of the spacecraft. In ZGM yaw angle pointing error is not negligible and therefore a simulation has been done in order to assess the behaviour of the Doppler frequency with different yaw error angles. The simulation has been done by analysing the Doppler residual shift due to a series of isolated point target across the swath. For each point target the residual Doppler defined in (1) had been computed.

$$F_{res}(\vec{V}_R, \vec{P}_i, yaw) = F_{th}(\vec{V}_R, \vec{P}_i, yaw) - F_{comp}(\vec{V}_R, \vec{P}_i) \quad (1)$$

Where \vec{V}_R is the relative velocity between satellite and target (i) and \vec{P}_i is the direction satellite-target (i).

In Yaw Steering Mode (YSM) and after an ideal on-board Doppler compensation the residual Doppler from each point target across the swath is roughly around 0 Hz. The introduction of a yaw error angle causes a frequency shift (because the ideal compensation law is computed only for yaw = 0°) that is function of the range (or of the echo sampling time). Fig. 3 and 4 show the residual Doppler for the Mid and Fore beam respectively at the ascending node (the Aft beam case is opposite, positive shift, to the Fore beam case due to the antenna acquisition geometry). The yaw error angle is ranging between 0 and 10 deg (with step of 0.5 deg). As shown in the figures, the evolution is not linear in particular for yaw errors angle above 2 deg. The residual shift is up to 30Khz for the Mid beam and up to 20 KHz for the Fore/Aft beam. It is interesting to note that the

Mid beam is more sensible to the yaw than the Fore/Aft beam To compute the "degree of non-linearity" the derivate of the residual Doppler across track had been computed. Fig. 5 and Fig. 6 show the first and second order derivate of the residual Doppler for the Mid beam while Fig. 7 and Fig. 8 show the same for the Fore beam case. The first order derivate is not perfectly constant across track in particular for high yaw error angle but the analysis of the second order derivate shows that there is a factor of 1.0E+3 between the two values. This means that, as first approximation, is possible to model the residual Doppler shift across track as a linear frequency shift (in particular for small yaw error angle) while for a full characterization of the evolution a second order polynomial is an appropriate model

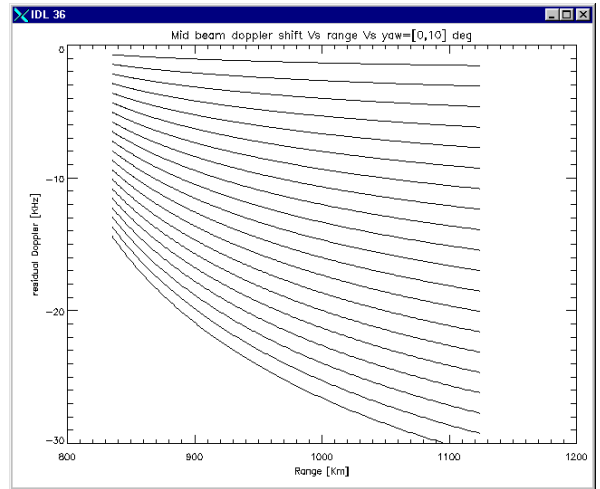


Fig. 3. Mid beam across track Doppler shift (with reference to ideal YSM) for yaw error angle ranging between 0° and 10° with a step of 0.5°.

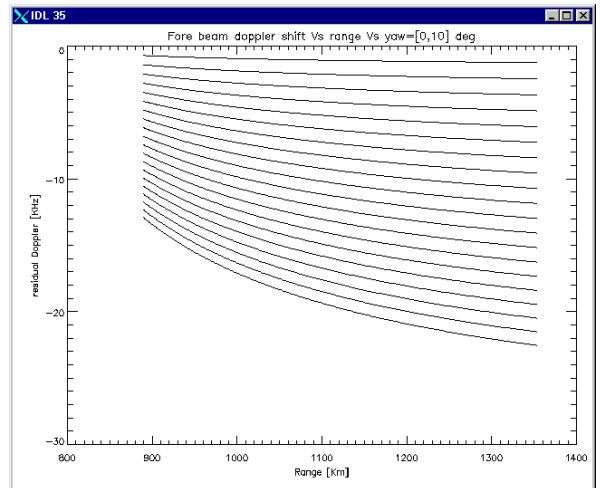


Fig. 4. Fore beam across track Doppler shift (with reference to ideal YSM) for yaw error angle ranging between 0° and 10° with a step of 0.5°.

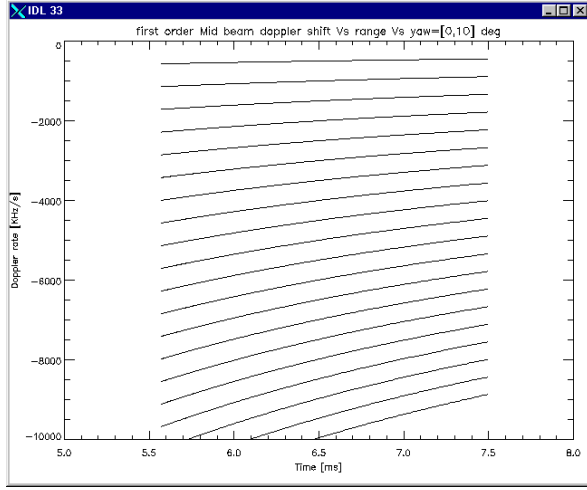


Fig. 5. Mid beam first order derivate of residual Doppler as function of the echo time for yaw error angle ranging between 0° and 10° with a step of 0.5° .

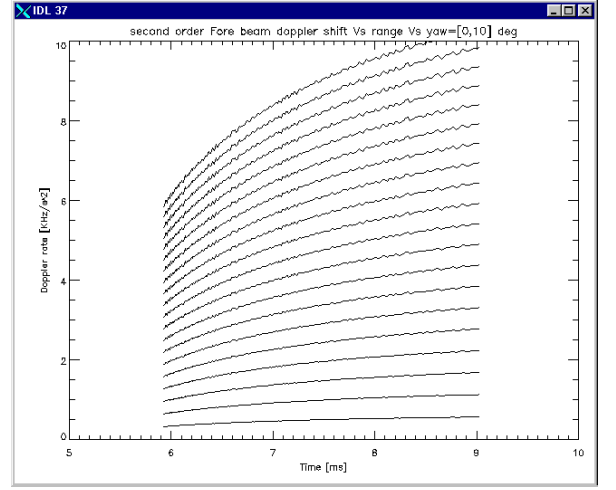


Fig. 8. Fore beam second order derivate of residual Doppler as function of the echo time for yaw error angle ranging between 0° and 10° with a step of 0.5° .

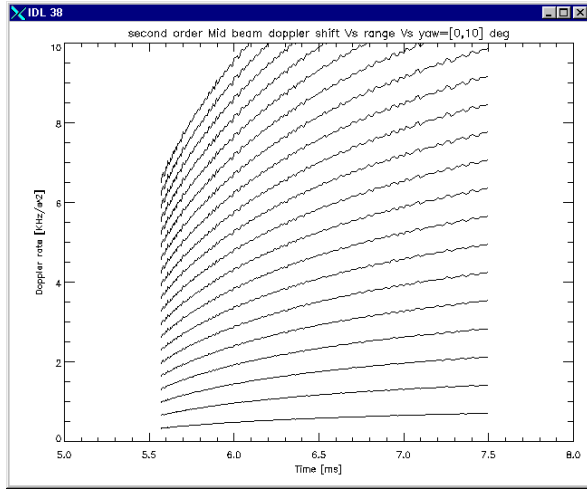


Fig. 6. Mid beam second order derivate of residual Doppler as function of the echo time for yaw error angle ranging between 0° and 10° with a step of 0.5° .

The error between the real Doppler frequency shift and the model can be defined as in (2)

$$\varepsilon = F_{res}(\bar{V}_R, \bar{P}_i, yaw) - (CoG + F_M \tau + F_{MM} \tau^2) \quad (2)$$

where τ is the echo time and CoG , F_M and F_{MM} are the model parameters. Fig. 9 and Fig.10 show the error evolution in the case of linear model respectively for the Mid and Fore beam case. The two parameters of the linear approximation (CoG , F_M) had been derived by a linear fit (minimum root square error) of the residual Doppler frequency across track. It is clear from the figures that the linear model performs a good fit in particular for the Fore/Aft case with an error up to 1.5 KHz for an error angle of 10° . For comparison Fig. 11 shows the error in the residual Doppler in the case of second order model (3 parameters used for the fit). In that case the error is up to 0.4 KHz.

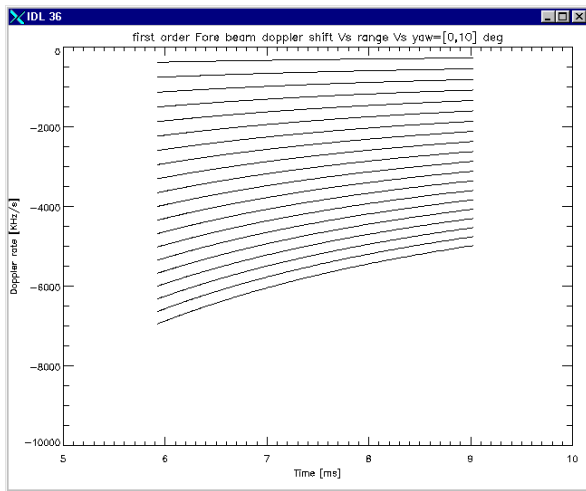


Fig. 7. Fore beam first order derivate of residual Doppler as function of the echo time for yaw error angle ranging between 0° and 10° with a step of 0.5° .

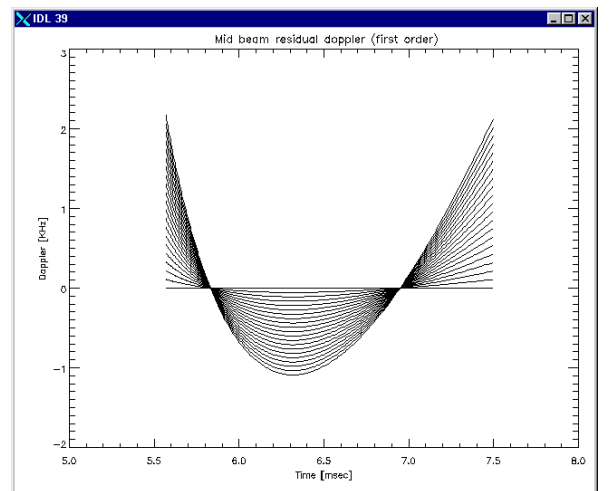


Fig. 9. Mid beam Model error first order approximation across track.

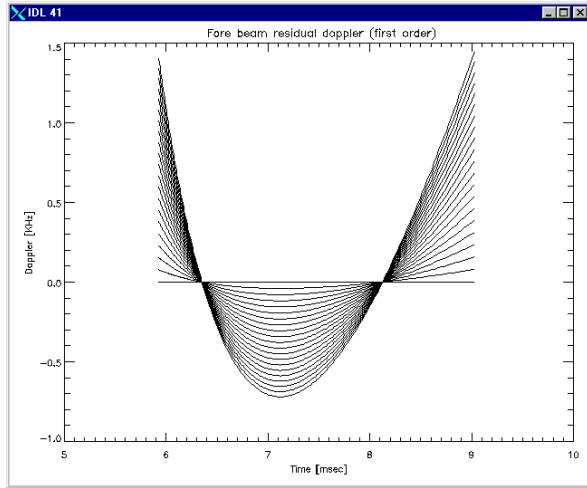


Fig. 10. Fore beam Model error first order approximation across track

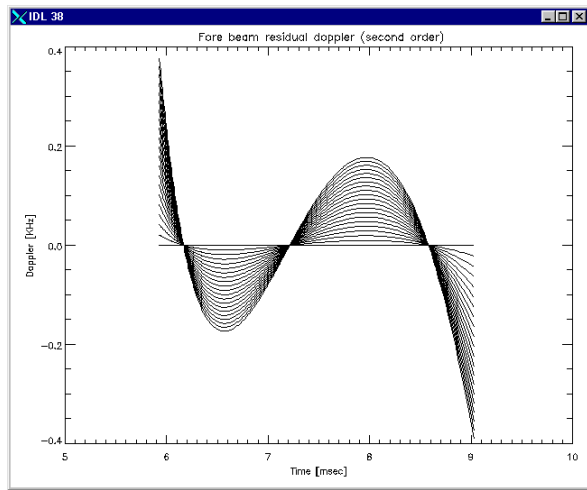


Fig. 11. Fore beam Model error second order approximation across track

2.3 The First Order approximation (Linear frequency modulation)

The analysis carried out in the previous section shows that in general the second order polynomial (parabola) is a "good" model to describe the additional Doppler variation (due to a yaw error angle) for a series of target point across the swath. The linear model is suitable for small yaw angle. For a given orbit time T the Scatterometer received signal is modulated according to:

$$T_{Rec}(\tau, yaw) = T_{Scat}(\tau) * h(yaw, \tau) \quad (4)$$

where:

τ is the echo time

$T_{Scat}(\tau)$ is the backscatter signal from the natural target

$h(yaw, \tau)$ is the modulating kernel due to the yaw error angle

If we assume for the kernel a linear model, only two parameters (function of both echo time and yaw) are

needed for a full characterization of the kernel itself. In particular we can define those parameters as an initial frequency F_i and a "compression factor" called Fm_rate (using a name from the SAR community) describing the slope of the linear modulation. The relationship between the yaw error and the parameters of the linear interpolation is reported in Figure 12 and Figure 13. Those figure show (solid line) the near range (initial frequency) and far range frequency (Y axis) against the slope (Fm rate) for the Mid and Fore antenna respectively. Different Fm_rate corresponding at different yaw error angle. Note that for a yaw error angle equal to 0 deg the curves go trough zero (no additional modulation due to a yaw error) because the kernel actually describes only the contribution of the yaw angle to the signal. As reported in the figures the position of the initial frequency shifts and the Fm_rate increases with the yaw.

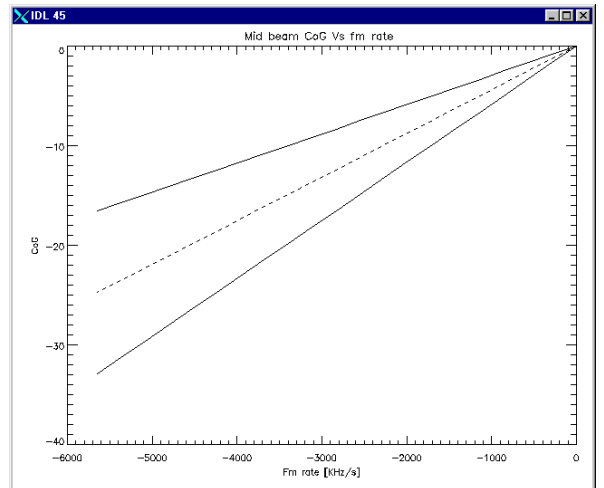


Fig. 12. Mid beam near range, far range as function of Fm rate (solid line)

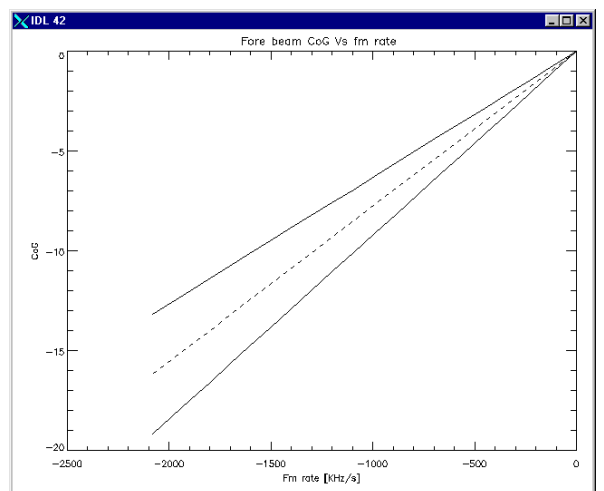


Fig. 13. Figure 10 Fore beam near range, far range as function of Fm rate (solid line)

2.4 The Kernel's Spectrum

One advantage of using a linear model (in the time domain) for the Kernel is that its spectrum is known. Equation (4) in the frequency domain becomes a convolution between the spectrum from the natural target and the kernel describing the yaw effect as in (5):

$$S_{Rec}(f, yaw) = \int_{-\infty}^{+\infty} S_{Scat}(f) * H(yaw, f - F) dF \quad (5)$$

The spectrum of the Kernel is [2] (6):

$$H(f) = \frac{1}{2} \sqrt{\frac{\tau}{2\mu}} \exp\left(-j\pi\tau\mu\left(\frac{f_i - f}{\mu}\right)^2\right) \{ [C(x_2) + C(x_2)] + j[S(x_2) + S(x_2)] \} \quad (6)$$

where:

$$C(y) = \int_0^y \cos\left(\frac{\pi}{2}x^2\right) dx$$

$$S(y) = \int_0^y \sin\left(\frac{\pi}{2}x^2\right) dx$$

τ is the length of the pulse

μ is the bandwidth

f_i is the initial frequency

The relationship between the Fm_rate and the spectrum bandwidth is the following:

$$\mu = 2 * \tau * (Fm_rate) \quad (7)$$

$\tau = 2.44$ ms (or 3.91 ms fore/aft case)

where Fm_rate is a function of the yaw angle.

As consequence of the convolution, the received spectrum is centred on the kernel's spectrum and its bandwidth is widened. The spectrum widening is proportional to the frequency shift and therefore to the yaw. Applying the linear model for a yaw error angle of 2 deg. the Fm_rate is 1.7 Mhz (Mid beam) and the bandwidth of kernel is roughly 8 KHz. In the case of the Fore/Aft beam we obtain for the Fm_rate a value of 676 KHz and for the Kernel's bandwidth a value of roughly 5.2 KHz. Those number show that with the same yaw error angle the modification of the Mid beam spectrum is more evident than the Fore/Aft one. This means that the yaw angle has a different impact depending on the antenna. The Figures 14 and 15 show the Kernel's spectrum (only positive frequency) for different yaw angles for the Mid and Fore antenna respectively. The spectrum has been computed in the bandwidth of the ERS-2 Scatterometer onboard receiver (± 12.5 KHz) taking into account the sampling frequency of 30KHz (the one used on-board). From the figures is clear the different behaviour of the Kernel respect to the antenna.

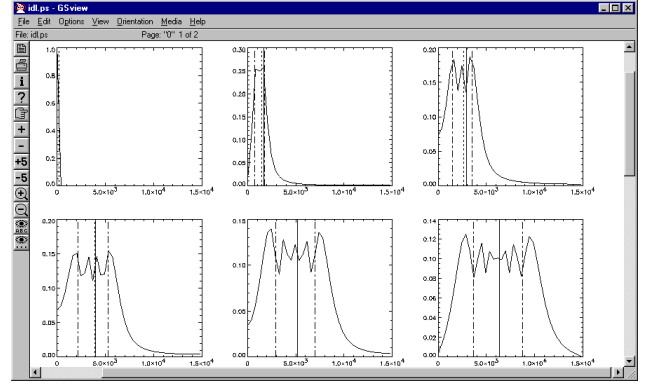


Fig. 14. Figure 11 Mid beam Kernel's Spectrum (one side) for yaw angle ranging between $[0^\circ - 2.5^\circ]$. Sampling frequency 30 KHz.

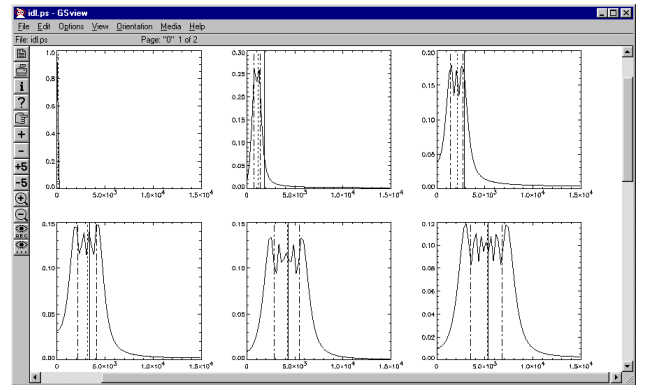


Fig. 15. Fore/Aft beam Kernel's Spectrum (one side) for yaw angle ranging between $[0^\circ - 2.5^\circ]$. Sampling frequency 30 KHz.

2.5 Upper limits for the yaw error angle

From the previous paragraph it is clear that a large yaw error angle produces a strong modification of the received spectrum. In principle that effect is not negative and could be compensated for on the ground processing if the yaw angle is known. In the real case of the ERS-2 Scatterometer the onboard receiver bandwidth is 25 KHz therefore to avoid loss of signal the result of the convolution (5) shall stay within the receiver bandwidth. As known the convolution between a spectrum with a bandwidth of B1 with a kernel with bandwidth B2 is a spectrum with a bandwidth of B1+B2. Moreover if the kernel is centred on a frequency F_0 the total bandwidth of the spectrum becomes B1+B2 +2* F_0 . In the case of the ERS-2 Scatterometer we have the following constraint (8):

$$B1+B2+2* F_0 = 25KHz \quad (8)$$

The bandwidth of the received signal B1 in nominal YSM is roughly 5 KHz centred around 0 Hz, this means that the contribution of the term B2+2* F_0 shall not exceed 20 KHz. Above that limit some of the received spectrum will be out of receiver and definitely lost. The Figure 16 shows the evolution of B2+2* F_0 against the

yaw error angle. The 20 KHz limit is reached for a yaw error angle of 1.5 deg (absolute value, or 3.0 peak-to-peak). The Figure 17 shows the result for the Fore/Aft case. The 20 KHz limit is reached for a yaw error angle of 2.5 deg (absolute value, or 5.0 deg peak-to-peak). As expected the result is more critical for the Mid beam than for Fore and Aft antenna.

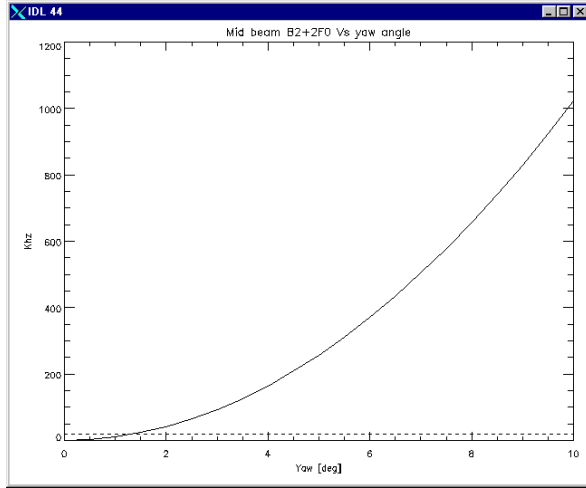


Fig. 16. Mid beam spectrum widening as function of yaw angle. Y axis scale KHz.

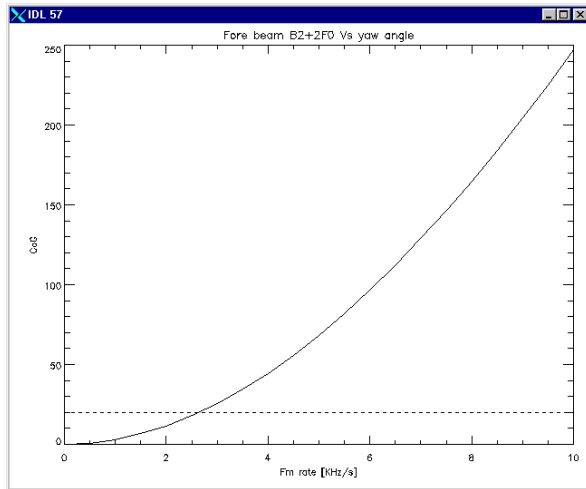


Fig. 17. Fore/Aft beam spectrum widening as function of yaw angle. Y axis scale KHz.

3. EFFECT OF YAW ANGLE ON RADAR EQUATION AND ECHO SAMPLE LOCALIZATION

A general description of the ERS Scatterometer ground processing is in [3]. The actual processor had been designed to fulfil the "fast delivery" constraint to provide wind data to user within 3 hours after acquisition. For that reason and taking into account a stable platform attitude (as reported in Table 1) many of normalization factors are pre-computed and supplied externally as Look-Up-Table (LUT) indexed by the orbit time and echo time. Scope of the chapter is to analyse

the error due to a yaw angle in the parameters of the radar equation and in the localization of the echo samples.

3.1 Radar Equation

The radar equation for distributed targets describes the received power modulated with the 2-way-antenna gain and with the reciprocal value of $\sin(\theta_i)$, where θ_i is the local incidence angle. These quantities are therefore dependent on the radar look angle θ_L , the depression angle of the antenna γ , the sensor position and attitude, the position of the backscatter element. [4]

The power received by the instrument on board is the approximately:

$$P(t, T) = k \frac{G_A^2(\gamma(R(t, T)))}{R^3(t, T) \sin(\theta_i(R(t, T)))} \quad (9)$$

Since the quantity to be measured is the backscatter coefficient σ^o , the measured power needs to be converted to σ^o . The Normalization factor N is defined as the instantaneous power for a uniform reference backscatter coefficient $\sigma_{ref}^o = 1$ on the earth surface everywhere in the swath. Due to the changing geometry with echo time t and orbit time T the normalisation coefficient N is a function of both t and T

$$N = N(t, T) \quad (10)$$

Knowing the normalisation coefficient, the σ^o value corresponding to t, T is determined by

$$\sigma^o(t, T) = \frac{P(t, T)}{N(t, T)} \quad (11)$$

$N(t, T)$ is dependent on the system geometry and on instrument and ground processing parameters. The quantities that change with a yaw angle are G_A^2 and $\sin(\theta_i)$ and only they are considered in the following study. The normalized antenna gain is defined, in the antenna reference frame, as a function of elevation angle θ and azimuth angle ϕ relative to the 1-way antenna gain in a reference look direction of the antenna. The normalized antenna pattern is defined via definition of azimuth and elevation cut. The normalized 1-way antenna gain is determined by:

$$G_N(\theta, \phi) = G_N(\theta, \phi_{AC}) \cdot G_N(\theta_{AC}, \phi) \quad (12)$$

Where:

θ : elevation angle

- ϕ : azimuth angle
- θ_{AC} : centre in antenna frames (elevation)
- ϕ_{AC} : centre in antenna frames (azimuth)

The sample position on the Earth's surface, and therefore elevation angle and azimuth angle associated to it, is yaw dependent. Consequently the Antenna Gain is influenced by yaw error angle. The Figure 18 (Mid beam), Figure 20 (Fore beam) and Figure 21 (Aft beam) show that influence. They have been done for some sample across the swath (different elevation angle). The curves represent the difference in dB between antenna gain in absence of yaw error angle and antenna gain in presence of a yaw error angle ranging between 1 and 5 degrees. The Figures show that the differences are smaller near to the ascending and descending node and near to the poles. In these points the differences in the elevation angle also are smaller (Fig.19 (Mid beam)-Fig.21 (Fore beam)-Fig.23 (Aft beam)).

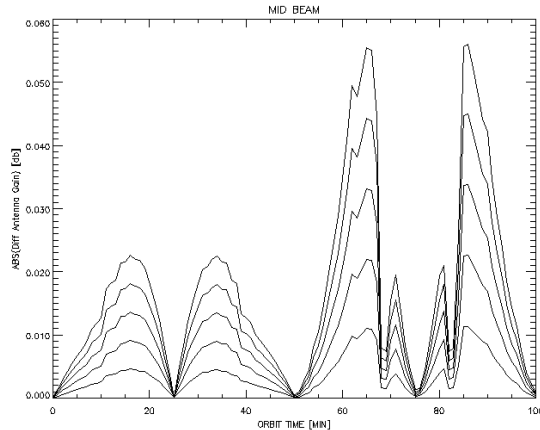


Fig. 18. *Mid beam*: absolute difference in Antenna Gain in function of Orbit Time and Yaw Angle ranging between 1 and 5 degrees for echo sample number 7 (near range).

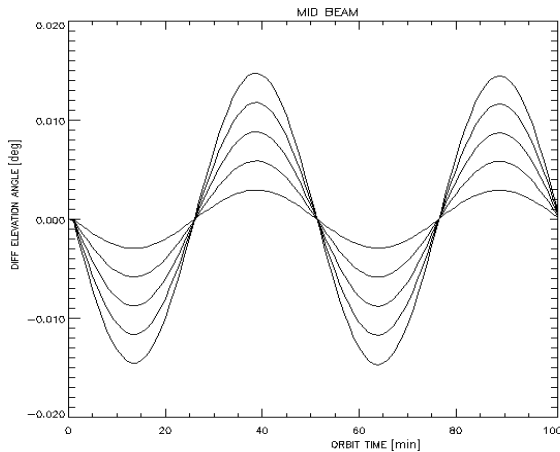


Fig. 19. *Mid beam*: absolute difference in Elevation Angle in function of Orbit Time and Yaw Angle ranging between 1 and 5 degrees for echo sample number 7 (near range).

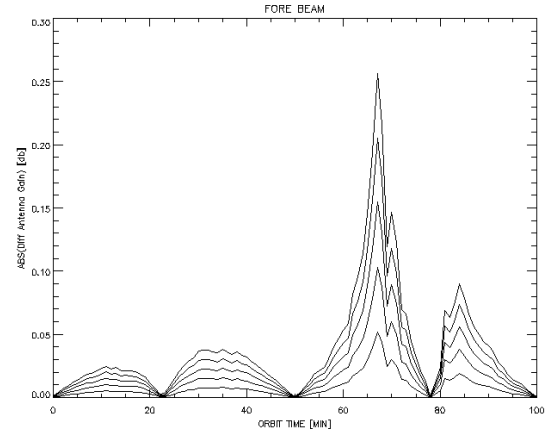


Fig. 20. as Fig. 18 Fore beam for echo sample number 2.

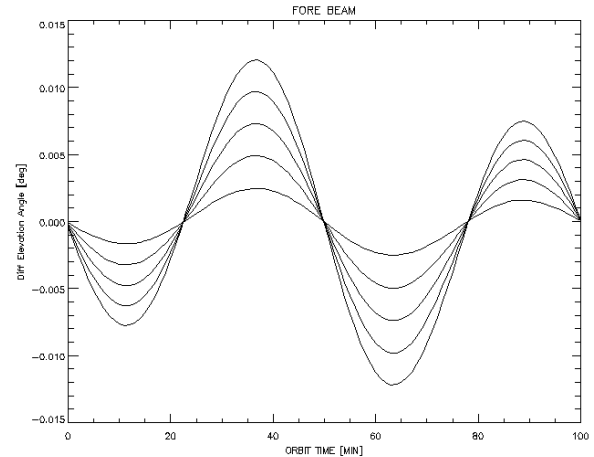


Fig. 21. as Fig 19 Fore beam for echo sample number 2.

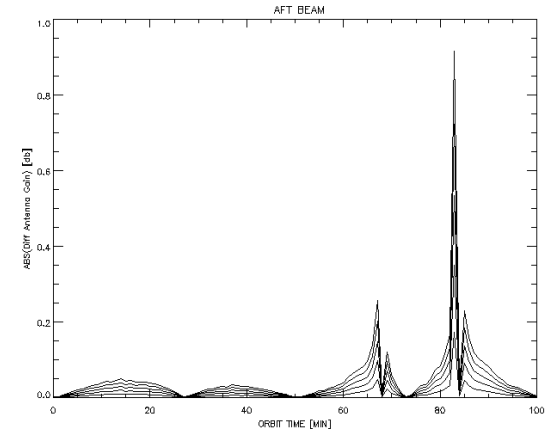


Fig. 22. as Fig 18 Aft beam for echo sample number 2.

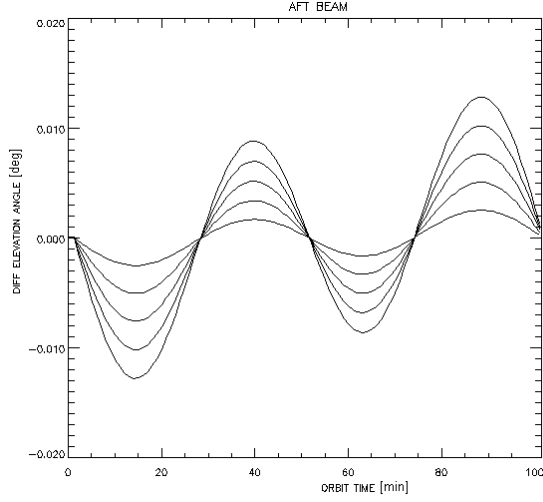


Fig. 23. as Fig 19 Aft beam for echo sample number 2.

The following figures show the difference in Antenna Gain in function of the Sample (across swath) and Yaw Angle. They have been done for some values of Orbit Time. The Figure 24 shows the behaviour for the Mid Beam. The Yaw Angle changes between 0 and 5 deg with step of 1 deg.

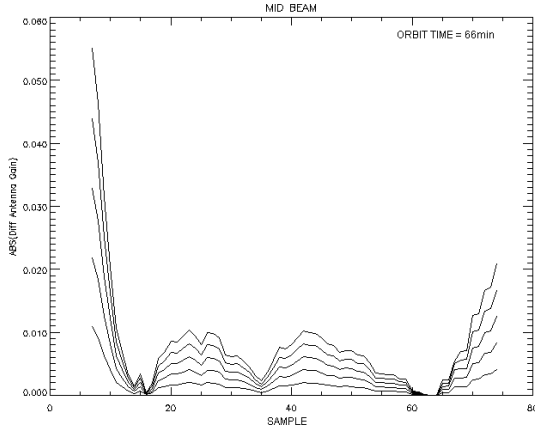


Fig. 24. Mid beam: absolute difference in Antenna Gain as function of number of sample for a Yaw Angle ranging between 1 and 5 degrees.

The Figures 25 and 26 show the same for the Fore Beam and Aft Beam. The result is a difference function of the sample number with a greater value at the near range.

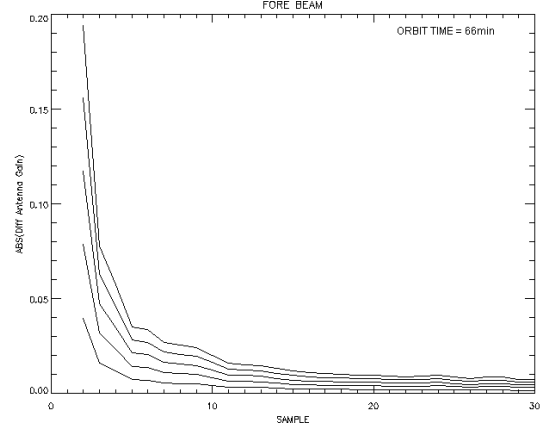


Fig. 25. Fore beam: absolute difference in Antenna Gain as function of number of sample for a Yaw Angle ranging between 1 and 5 degrees.

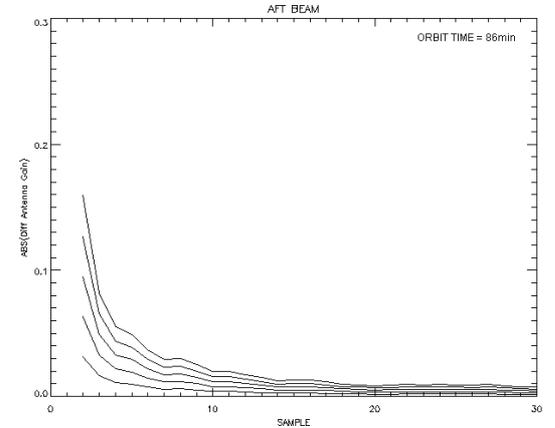


Fig. 26. Aft beam: absolute difference in Antenna Gain as function of number of sample for a Yaw Angle ranging between 1 and 5 degrees.

The incidence angle at a point $\underline{P}(x,y,z)$ on the earth surface is defined as the angle between the vector \underline{r}_{SC-P} connecting satellite and \underline{P} and the normal vector in \underline{P} , \underline{N}_P :

$$\theta_i = a \cos \left(\frac{\underline{r}_{SC-P} \cdot \underline{N}_P}{\|\underline{r}_{SC-P}\| \cdot \|\underline{N}_P\|} \right) \quad (13)$$

Obviously the incidence angle is yaw dependent. The Figures 27-28-29 (Mid, Fore and Aft) show the influence on SIN of Incidence Angle. The curves represent the difference in db between sin of Incidence Angle in absence of yaw error angle and sin of Incidence Angle in presence of a yaw error angle. The Yaw Angle ranges between 1 and 5 deg with steps of 1 deg. The Figures show that there are no large differences in the $\sin(\theta_i)$. This factor is always less than $1.5 \cdot 10^{-4}$ dB.

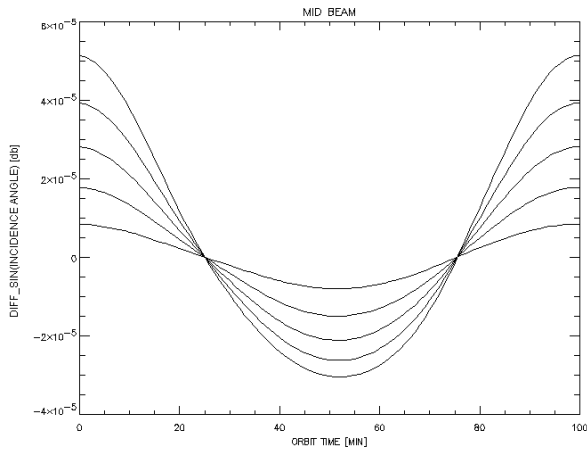


Fig. 27. *Mid Beam*: difference in Sin of the Incidence Angle in function of the Orbit Time and Yaw Angle ranging between 1 and 5 degrees for 7th sample.

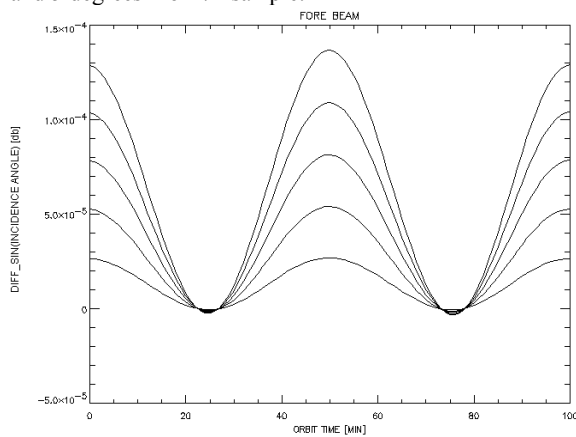


Fig. 28. *Fore Beam*: difference in Sin of the Incidence Angle in function of the Orbit Time and Yaw Angle ranging between 1 and 5 degrees for 1st sample.

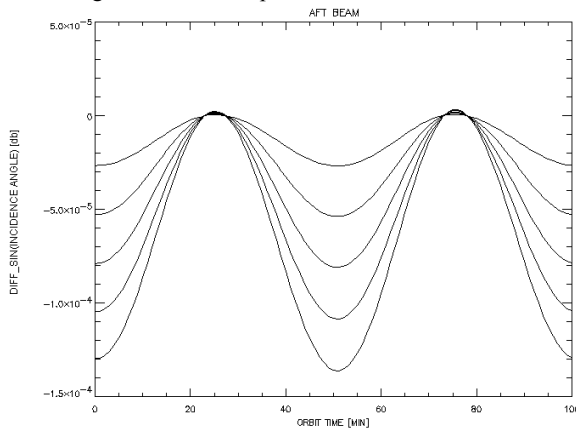


Fig. 29. *Aft Beam*: difference in Sin of the Incidence Angle in function of the Orbit Time and Yaw Angle ranging between 1 and 5 degrees for 1st sample.

According with the previous graphs a yaw estimation error has a very small influence on Incidence Angle (less than 0.003° with yaw error angle of 5°) and Elevation Angle (less than 0.015° with yaw angle of 5°). On the contrary the yaw error angle has an influence on the antenna gain not negligible. The antenna gain graphs

show that the effect of the yaw error angle is large only for some values of orbit time and for the first samples.

3.2 Localization of the echo sample

As reported in [1] the position of the nodes inside the swath is relative to the intersection between the mid beam antenna boresight with the reference ellipsoid. The actual processor makes the assumption that no degradation is in satellite attitude so the samples that contribute to a node are selected by a pre-computed table. The introduction of a yaw error angle modifies the set of samples used to generate a node. This behavior is shown in Figure 30 (Fore beam) Figure 31 (Mid beam) and Figure 32 (Aft beam). According with those Figures the sample pre-selection, performed in the actual ground processing, leads to an error in particular for the far range nodes.

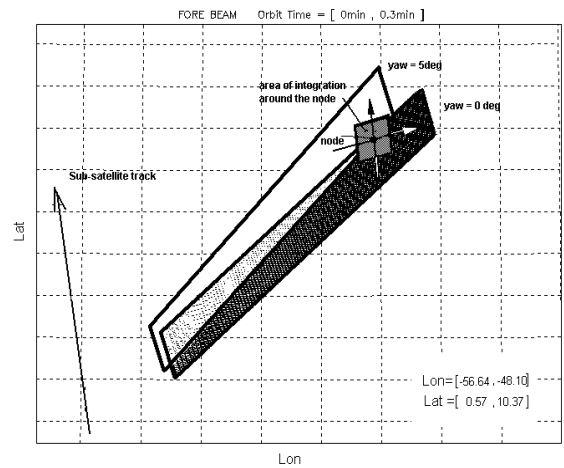


Fig. 30. *Fore beam*: samples in absence of yaw error (black area) and same samples with a yaw error of 5 deg. (white area) for 15 sec of along track data around the ascending node.

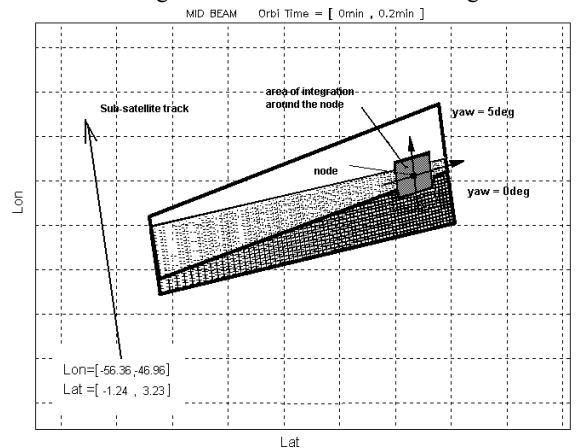


Fig. 31. *Mid beam*: as For Fig 30 Mid beam case.

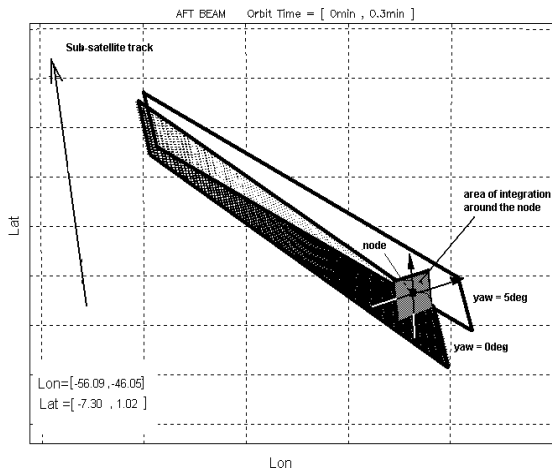


Fig. 32. Aft beam: samples in absence of yaw error (black area) and same samples with a yaw error of 5 deg. (white area) for 15 sec of along track data around the ascending node.

3.3 The Sigma Nought error in the UWI data

The UWI (User Wind) are the final product of the Scatterometer ground processor and are the data distributed to the users. Those data contain sigma nought measurements (for each antenna) as well as the retrieved winds (speed and direction). Figure 33 shows the comparison between sigma noughts acquired in nominal YSM and sigma noughts acquired in Fine Pointing Mode (FPM) for the same relative track. In FPM the yaw correction reported in Figure 1 is not applied to the satellite therefore data are acquired with a yaw error angle ranging between ± 4 degrees. As shown in that figure the maximum error angle is achieved at the crossing node (ascending and descending) for an orbit time of 0sec and 3000 sec. In the figures the asterisks are indicating the sigma noughts acquired in FPM. The data acquired over the Land and over the Sea are respectively coloured in brown and in light blue. On the same figures the crosses and the diamonds are indicating the sigma noughts acquired in nominal mode over the same relative track, respectively one and two years before the FPM mode. The data acquired over the land are coloured in green (one year before the FPM data) and in red (two year before the FPM data); the data acquired over ocean are coloured in dark blue. The Figure 33 clearly shows the impact of the yaw error angle. In particular roughly 3000 seconds after the ascending node the satellite was over the Amazonian Rain Forest that is a stable target. In fact the same passage after one year shows the same sigma noughts (green and red data are overlapping). The data acquired in FPM with an error angle of 4 degrees are clear degraded. In fact the sigma noughts are lower than the nominal (up to 5 dB for the Far range nodes). The degradation is also function of the incidence angle. The differences over the sea are less clear due to the variability of the ocean surface due to the wind but it is also present in particular around the ascending node

(around 0 sec) where the yaw error is 4 degrees. In that part of the orbit there is a clear reduction of the sigma noughts that is not related with geophysical effect.

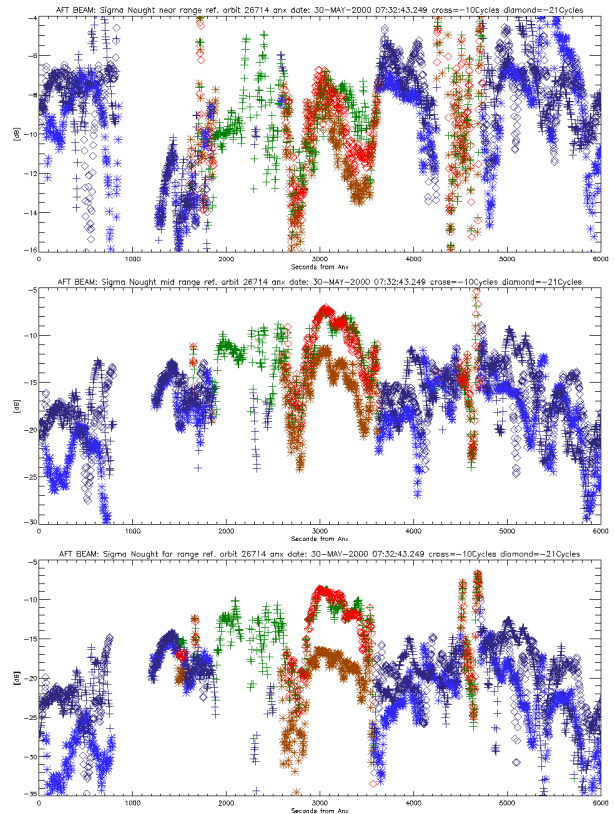


Fig. 33. ERS Comparison between Scatterometer Aft Antenna Sigma Noughts as function of the ascending node time acquired in nominal YSM and without the yaw error angle correction. Upper panel Near Range, mid panel Mid range, lower panel Far range.

4. CONCLUSIONS

The effect of a yaw error angle on the Scatterometer signal has been modelised in the frequency domain as a convolution with a Kernel that performs a linear frequency modulation.

The parameters of that modulation (the initial frequency and the Fm rate) are function of the yaw angle and of both echo and orbit time. The impact of that convolution is that the received spectrum is shifted and widened if compared with the one acquired in nominal mode (without yaw error).

In principle the spectrum modification could be compensated for in the ground processing by estimating the yaw error angle. A limit for such correction arises

from the ERS Scatterometer instrument itself. In fact the receiver bandwidth is 25 KHz and therefore any signal shall be inside that band to avoid a final loss of information. The simulation performed shows that the Mid beam is the most critical case. For that beam the bandwidth of the Kernel reaches the maximum of 25 KHz with a yaw error angle within ± 2.5 degrees. This seems the acceptable limit to re-process the data with a new algorithm that takes into account the yaw error in satellite attitude as reported in ^[5].

5. REFERENCES

- [1] ERS-2 Satellite to ground segment interface specification ER-IS-ESA-GS-0002 p 3-19
- [2] G. Picardi "Elaborazione del segnale radar" Franco Angeli 1988 pp 146-152
- [3] P. Lecomte "The ERS Scatterometer instrument and the on-ground processing of its data" proceeding of Emerging Scatterometer Application workshop ESA-SP-424 pp 241-260
- [4] Holecz F. et al., Rigorous Derivation of Backscattering Coefficient, IEEE Geoscience and Remote Sensing Society Newsletter 1994, N.92.
- [5] X. Neyt, P. Pettiaux, M. Acheroy "Scatterometer Ground Processing Review for Gyro-Less Operations" proceeding of 9th International Symposium on Remote Sensing, Crete, Greece 22 - 27 September 2002